



AERODYNAMIC STABILITY OF ADDITIVELY MANUFACTURED HEXA-COPTER FRAME

Mohammad Abdul Fazal¹, Research Scholar, Department of Mechanical Engineering, Osmania University, Hyderabad, Telangana, India.

Prof. A. Rajasekhar², Head of the Department, Mechanical engineering, Methodist College of engineering and technology, Hyderabad. Telangana, India.

Prof. R. Rajendra³, Department of Mechanical Engineering, Osmania University, Hyderabad, Telangana, India.

¹abdulfazal7@gmail.com, ²hodmech@methodist.edu.in, ³regaraj@gmail.com

Abstract The aerodynamic stability of a Hexa-Copter drone frame that was designed using additive manufacturing techniques, specifically Fused Deposition Modeling. The drone frame is made up of hollow square cross-sectional arms optimized for structural integrity through Finite Element Analysis and topological optimization. Carbon Fiber Reinforced Polymer is embedded in the design for high strength with a low weight ratio to enhance the performance of the frame. Additive manufacturing allows for the possibility of better design flexibility and precision than traditional manufacturing techniques can achieve, hence the capability for complex geometries and light structures. Slicing for 3D printing was done in Ultimaker Cura software. Computational Fluid Dynamics (CFD) simulations were performed to predict the aerodynamic performance of a Hexa-Copter configuration under different angles of attack during forward flight conditions. The drag forces calculated by CFD were validated in the wind tunnel at different speeds. A comparative analysis between numerical and experimental results shows a good correlation that reveals the enhanced aerodynamic stability of the Hexa-Copter and Strain measurement process. The results show that higher AoA and maximum cross-sectional area provide the best performance of the drone, reflecting the robustness of an aerodynamic design that is efficient in flight stability.

Keywords: Aerodynamic Stability, Additive Manufacturing, Fused Deposition Modeling (FDM), 3D Printing, Topological Optimization, CFD Simulation.

1. Introduction

The rapid growth in the field of unmanned aerial vehicles, specifically hexacopter, has made them quite popular in many fields such as agriculture, disaster management, and aerospace engineering. A lot of analysis has been carried out with the aim of optimizing the aerodynamic efficiency and structural integrity of hexacopter. The studies conducted on the aerodynamic performance of hex-rotor UAVs in several conditions have gained important knowledge regarding their functionality [2], [6]. Similarly, CFD simulations have been used in the validation of experimental results with further optimization of design parameters [3], [8], [19]. Introduction of additive manufacturing techniques in the design of UAVs has enabled the fabrication of lightweight, high-strength components that help in increasing payload capacity and generally improving the performance of UAVs [4], [11], [13]. Recent works have emphasized the application of 3D printing for topologically optimized structural parts manufacturing, such as wing spars and frames, using carbon fiber-reinforced composites [5], [12], [18]. These contributions have paved the way toward the optimal design of UAVs for dedicated missions related to disaster management and chemical detection [7], [16]. This research on the design of UAVs, including hexacopter, has been further extended by investigating flight dynamics and stability in changing environmental conditions. Indeed, it has been established that state and disturbance observers are effective in maintaining control stability in terrestrial hexacopter [33] and mechanisms of tethered power have been put forward as a means of extending durations airborne [34]. These further underline the integration of aerodynamic efficiency, advanced materials, and control systems in modern UAV design [14], [32]. This has included specific concentration on the use of UAVs for agricultural purposes, testing their suitability for pesticide application and payload-based operations [10], [35]. More recent wind tunnel tests on UAV rotor performance under icing conditions further underline the importance of environmental considerations for UAV operation [28]. Continued design development of hexa-

copter for high payload capacity applications underscores their commercial and industrial potential [27], [31]. The present study discuss recent progress made in design development concerning hexacopter systems, where attainment of high performance and versatility can be attributed to synergetic improvements in aerodynamics optimization, material sciences, and control systems.

2. Materials and Methods

CFRP is a composite material made of carbon fibers in a polymer matrix. The carbon fibers impart strength and rigidity, while the polymer matrix is normally from epoxy or other resins that bind the fibers together. Because of its great strength-to-weight ratio, CFRP has become an important material in aerospace, automotive, and other engineering applications when mass needs to be low and strength high. The carbon fibers are oriented in specific directions to optimize performance in certain loading conditions, therefore enhancing the overall mechanical properties of the composite. Nylon 6/6 (Polyamide 6/6): Nylon 6/6 is a synthetic polymer belonging to the family of polyamides. It has excellent mechanical properties such as high tensile strength, good chemical resistance, and dimensional stability. It is also used in such applications where toughness is needed, including automotive parts, electrical equipment, and textiles. In the context of CFRP, Nylon 6/6 may be used as part of the matrix material, providing added toughness, thermal stability, and resistance to wear and friction. CFRP combined with Nylon 6/6 forms a composite material that exploits the synergy between carbon fiber light weight and strength, while Nylon 6/6 provides toughness and durability. This combination has been used in drone components, automotive parts, and other systems that require both high strength and impact resistance. This material combination is designed with the purpose of enhancing structural integrity, reducing weight, and improving performance under dynamic conditions [35] [36] [37].

Table.1. Mechanical properties of the material

S. No	Property	Values
1	Material	CFRP
2	Mass density (kg/m ³)	1170
3	Poissons ratio	0.4
4	Young's modulus (MPa)	7453
5	Ultimate tensile strength (MPa)	81.7
6	Compressive strength (MPa)	500
7	Yield strength (MPa)	49.02
8	Flexural strength (MPa)	169
9	Elongation at break (%)	3

The proposed research methodology for the study of the Hexa-copter drone combines computational and experimental approaches to analyze its aerodynamic performance and structural optimization. First, a structural analysis of the Hexa-copter frame with hollow square cross-sectional arms is performed using FEM to determine its load-carrying capacity. Then, topological optimization of the drone arm is performed based on maximum strength with minimum weight. The structural analysis of the optimized arm is then done with the inclusion of the properties of carbon fiber-reinforced polymer (CFRP) for better results. Fabrication of the frame of the drone will be done through additive manufacturing and specifically through Fused Deposition Modeling (FDM), which has substantial benefits compared to traditional methods as it enables easier and more viable manufacturing of complex UAV structures [1], [2]. After designing, slicing of the Hexa-copter model is done for 3D printing using Ultimaker Cura. CFD simulations were done for different AoA in the forward flight phase to assess the aerodynamic performance. Simulations analyze the flow of air around Hexa-copter and provide an approximate estimation of drag forces. Wind tunnel tests were conducted to validate results obtained from CFD. Tests were conducted at 8.22 m/s, 5.81 m/s, and 3.68 m/s wind speeds and corresponding drag values recorded. The goals of the wind tunnel test are to compare CFD-simulated drag forces with experimentally measured data. The wind tunnel simulates motion by blowing air around the stationary drone, replicating forward flight conditions of the

Hexa-copter. This comparative evaluation between numerical and experimental analyses for various wind speeds and angles of attack has shown good correlation, confirming the stability of the Hexa-copter design in real-world conditions [3] [4][5].



Figure.1.Drone Assemble Isometric View

Design for additive manufacturing is finding its wide adoption in industries because of its unparalleled feasibility and flexibility of manufacturing. Among all the techniques, the Fused Deposition Modeling process holds a unique advantage and can be considered ideal for the creation of complex structures. Unlike most traditional methods, which have constraints on design by the requirement of tooling, FDM offers ease in making complicated geometries. Such a capability is of special importance in the manufacturing of Unmanned Aerial Vehicle structures-for instance, drone frames-where lightweight yet robust design is very critical. This layer-by-layer fabrication of FDM will allow for efficient usage of material and customization, hence reducing cost and time considerably. Besides, FDM allows using advanced materials, like CFRP, which enhance strength-to-weight ratios of the components of UAVs. This process also simplifies prototyping and iterative design modification, enabling engineers to optimize structures for particular performance criteria. Generally speaking, FDM benefits in UAV manufacturing enable new paths for innovation, not only in aerospace but also in other high-performance applications.

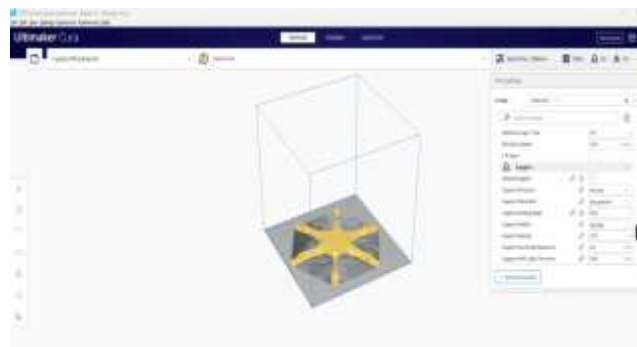


Figure.2. Hexa-Copter Sliced Using Ultimaker Cura

Table.2.Parameter and specifications for Ultimaker Cura

Parameter	Specification
Printer Type	DP600 Fused Deposition Modelling
Build Volume	600x600x600Corexy architecture
Extruder Type	Direct Drive-Single extruder
Nozzle Diameter	0.4 mm
Filament Compatibility	Material Supported like PLA, ABS, PETG, PLA-CF, CFRP
Bed Type	Heated Bed
Max Extruder Temperature	260° C
Max Bed Temperature	120° C
Max print temperature	300 °C
Max chamber temperature	80° C
Max Print Speed	150 mm/s



Figure.3.Hexa-copter drone 3D printing

Table.3.Printing Parameters

Parameter	Value
Material	CFRP-nylon
Layer Height	0.1 mm
Infill Density (%)	100 %
Infill Pattern	Rectilinear
Max Overhang angle for Support	45°
Support Infill (%)	15%
Support Infill Pattern	Zig-Zag
Printing Speed	60 mm/s
Nozzle Temperature (°C)	230



Figure.4.Manufacturing of Hexa-Copter Sliced using 3D printing

2.1 Aerodynamic Performance Measures of Developed Hexacopter Using Cfd and Wind Tunnel Testing

The aerodynamic performance of hexacopter is a very important factor in optimizing efficiency, stability, and payload capabilities, especially under variable environmental conditions. Two of the most widely used complementary approaches for the evaluation and improvement of hexacopter performance include Computational Fluid Dynamics and wind tunnel testing. CFD simulations can give a good overview of the flow dynamics, pressure distributions, and drag forces acting on hexacopter structures. For instance, optimized propeller blade designs demonstrated significantly improved thrust generation while reducing the associated aerodynamic losses [3]. Also, wind tunnel testing is necessary to validate CFD results under real flight conditions while enabling accurate measurements of lift, drag, and stability parameters [29]. The hexacopter, being designed with enhanced aerodynamic profiles, have streamlined rotor housings and optimized frame structures that lead to better energy efficiency and reduced turbulence-induced instability. Research has shown that, with advanced materials and structural optimization techniques adopted in recent hexacopter designs, air resistance is minimized and payload capacity enhanced [27] [35]. The horizontal airflow and variations in the angle of attack have been studied for their influence on aerodynamic performance, with the resulting understanding that these parameters bear much significance in flight stability and maneuverability [2] [9]. Wind tunnel investigations have highlighted several critical performance aspects during forward flight conditions, such as icing effects on rotor blades, which can drastically deteriorate thrust and efficiency in flight [28]. In addition, the integration of CFD-based trajectory control strategies ensures adherence to prescribed performance parameters by the hexacopter during dynamic operations [30]. These studies in juxtaposition bring out the importance of using CFD and wind tunnel testing to further the aerodynamic capability of hexacopter with superior performance and reliability over a wide range of operational scenarios.

Table.4.Mesh Statistics

Mesh Statistics			
Domain Name	Orthog. Angle	Exp. Factor	Aspect Ratio
	Minimum [deg]	Maximum	Maximum
Default Domain	20.1 ok	124 !	50 OK
	%! %ok %OK	%! %ok %OK	%! %ok %OK
Default Domain	0 6 94	<1 5 95	0 0 100

Simulations are done for Forward Phase at wind velocity 8.22 m/s, 5.81 m/s and 3.68 m/s and for Angle of Attacks 0°, 4°, 8°, 12°

1. For wind velocity 8.22 m/s the following Pressure & Velocity

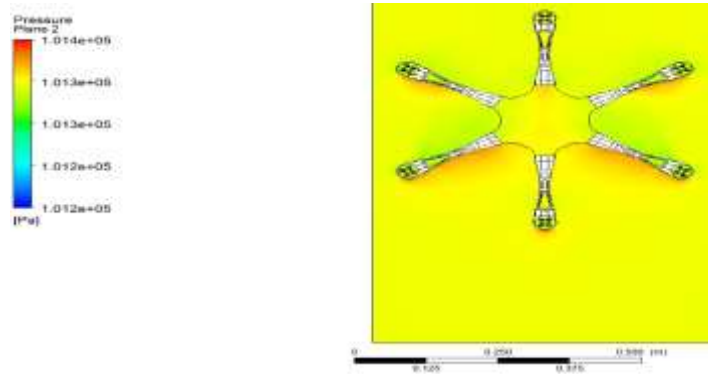


Figure.5. Pressure for AoA of 0°

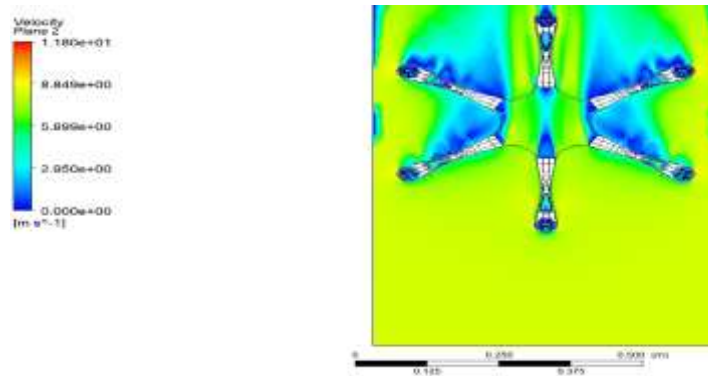


Figure.6. Velocity for AoA of 0°

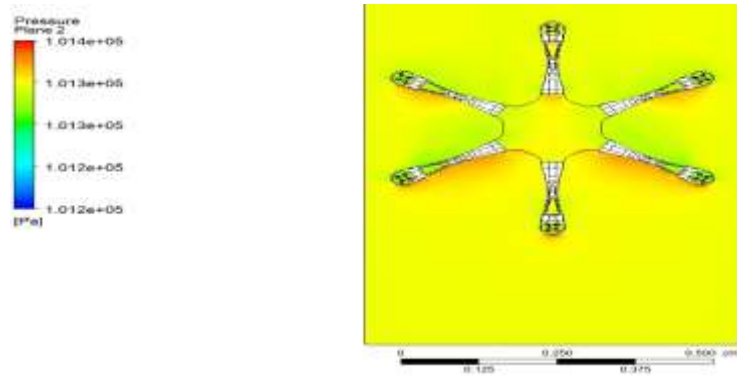


Figure.7. Pressure for AoA of 4°

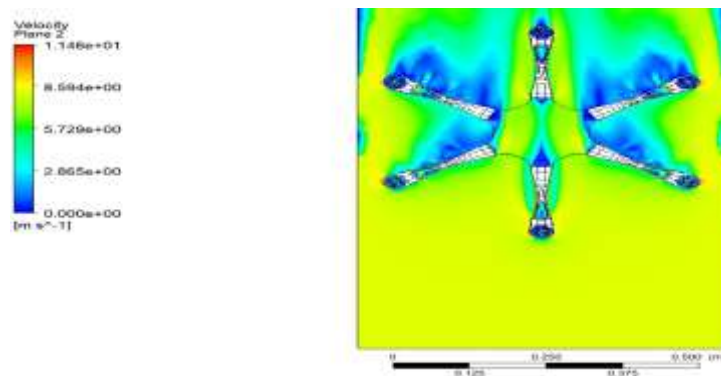


Figure.8.Velocity for AoA of 4°

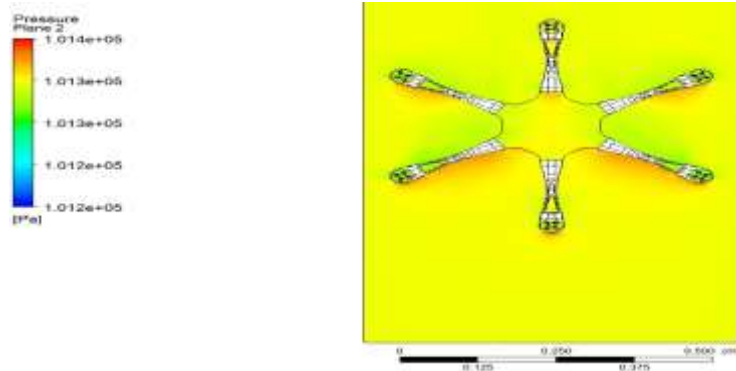


Figure.9.Pressure for AoA of 4°

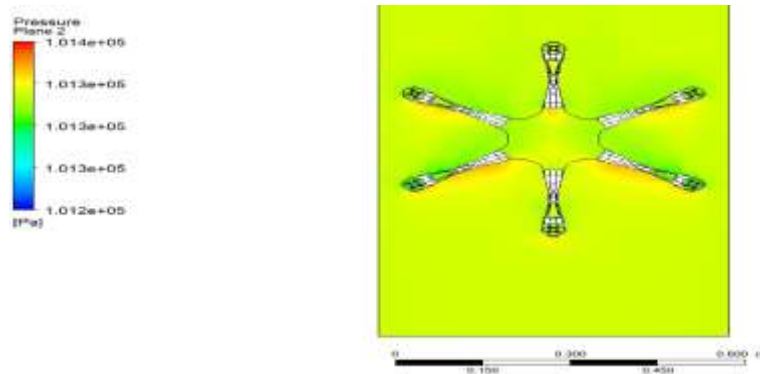


Figure.10.Pressure for AoA of 8°

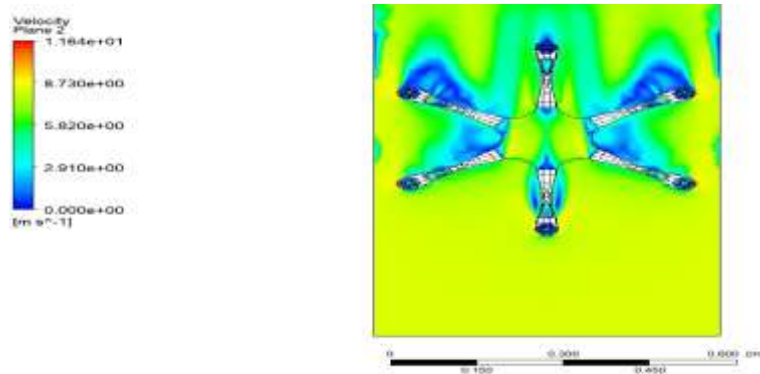


Figure.11.Velocity for AoA of 8°

Similarly simulations are done for remaining velocities of 5.81 m/s and 3.68 m/s and for Angle of Attacks 0°, 4°, 6°, 12° are done.

Wind Tunnel Testing: Testing in the wind tunnel is carried out for different speeds, i.e., 8.22 m/s, 5.81 m/s, and 3.68 m/s, and corresponding drag values calculated. The intent of the wind tunnel test is to validate the drag force obtained from the CFD analysis/simulation. Hence, forward condition simulations and wind tunnel test comparisons are made, since the chances of maximum drag force arising would be maximum for maximum cross-section area. Wind provided inside the wind tunnel will be equivalent to the velocity of Hexa-copter provided in simulations, i.e., instead of Hexa-copter flying against wind, wind is blown against Hexa-copter. The drag force, for this, is provided through rotation of propellers in the CFD simulation, whereas in the wind tunnel, the drag force is provided externally.



Figure.14.Wind tunnel

Table.5. Low Speed Wind Tunnel Specifications

Test Section Size	Cross Section: 600mmx600mm. Length: 2000mm.
Maximum Speed of Fan	50m/sec. Axial Flow fan of Diameter: 1.3 meter Maximum rpm: 1450 Number of Blades: 12 Hub Diameter: 500mm Spinner is provided
Contraction Ratio	9:1
Contraction length	1.8m
Settling chamber	1800mm x 1800mm
Entry section	Bell mouthed entry
Honey Comb Size	25mm x 25mm x 200mm
Screens	Two screens 8mesh and 6mesh stainless steel
Provision to put smoke rake	provided in the contraction cone.
Power	22KW AC motor, with speed control drive

2.2 Orientation of Hexa-Copter with Different Angle of Attacks (AoA) for Forward Phase



Figure.15.AoA of 0°



Figure.16.AoA of 8°



Figure.17.AoA of 12°

A comparative evaluation between numerical and experimental analyses at different wind speeds shows good correlation for various angles of attack. The drag results indicate that the drone exhibits higher stability.

2.3 Measurement of Strain in Hexa-copter Structure Using Strain Gauge

A strain gauge, a precision instrument, is used to measure the deformation of solid materials under stress. The bonded metallic strain gauge, known for its accuracy, is the most commonly used in applications like aircraft component testing [1]. The Wheatstone bridge, an important circuit, is used to measure resistance changes in strain measurement. It mainly has configurations like quarter-bridge, half-bridge, and full-bridge. The quarter-bridge configuration, widely applied due to its high sensitivity and simplicity, further enhances the precision of the strain gauge [3]. In the hexacopter structural strain study, the strain gauge is carefully mounted on the arm of the hexa-copter. The process involves fabricating the strain gauge using fused deposition modeling (FDM) and then using an adhesive to mount it directly onto the carbon-fiber-reinforced polymer (CFRP) material of the hexacopter arm. When in use, the thrust force squeezes the strain gauge itself, resulting in a resistance change that is proportional to the strain induced. This change in resistance is used to calculate the strain accurately [2], [6]. For this application, the 1-LY41-6/350 linear strain gauge was chosen due to its small size and compatibility. A quarter-bridge configuration is implemented by replacing one resistor in the Wheatstone Bridge with the strain gauge [5], [13]. The strain measurement system uses the Mx1615B strain gauge amplifier and Catman software for data acquisition and analysis to ensure accurate strain assessment in the hexacopter structure [9], [12]. This underscores the crucial role of the strain gauge in understanding the mechanical behavior of UAV components during operation, making the work of the engineers and researchers in this field even more significant.

Table.6 Specifications of Strain Gauge and Data Acquisition System

Model	MX1615B_CHT
Units	$\mu\text{m/m}$
Sensor	SG 4 wire 350 Ohm
Transducer type	SQ quarter bridge 350 Ohm, 4-wire circuit
Native unit	Native unit mV/V
Nominal range	0-8000 $\mu\text{m/m}$
Filter characteristics	Excitation: 5 V excitation
Zero balancing (0)	Filter frequency: 10 Hz
Bridge factor 0.00000	Gauge factor: 2.00000

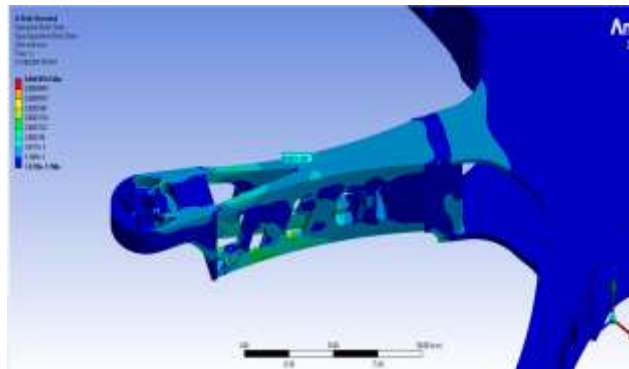


Figure.18 Strain at 50 % throttle

3. Results

Table.5. Simulation results for Forward Phase at a wind velocity of 8.22 m/s

AOA	Lift (N)	Drag (N)	Cl	Cd
0°	0.01979	0.687058045	0.001684	0.058455
4°	0.117078	0.719653009	0.009961	0.061229
8°	0.286557	0.85796809	0.024381	0.072997
12°	0.527979	0.99202335	0.044921	0.084402

With increased wind velocities, the lift and drag forces are seen to increase with the angle of attack. For instance, at 0° AOA, the lift force is 0.01979 N, while the drag is 0.687058045 N, with Cl and Cd values of 0.001684 and 0.058455, respectively. These are maximum when AOA = 12° the lift is equal to 0.527979 N, drag reaches 0.99202335 N, Cl - 0.044921, and Cd - 0.084402, which shows a clear improvement in force amplification with increased AOA.

Table.6. Simulation results for Forward Phase at a wind velocity of 5.81 m/s

AOA	Lift (N)	Drag (N)	Cl	Cd
0°	0.0077745	0.756197	0.001324	0.128783
4°	0.0357375	0.792239	0.006086	0.134921
8°	0.090789	0.9440355	0.015462	0.160772
12°	0.1634835	1.0917688	0.027842	0.185932

Therefore, in this case, with lower wind velocity, the aerodynamic forces are somewhat smaller. For 0° AOA, the lift and drag are 0.0077745 N and 0.756197 N, respectively, while corresponding values of Cl and Cd are 0.001324 and 0.128783, respectively. On the other hand, lift increases to 0.1634835 N at 12° AOA, while drag

increases to 1.0917688 N, and the respective values of Cl and Cd are 0.027842 and 0.185932, respectively, depicting similar trends as observed with higher wind velocities.

Table.7.Simulation results for Forward Phase at a wind velocity of 3.68 m/s

AOA	Lift (N)	Drag (N)	Cl	Cd
0 ⁰	0.005183	0.138278	0.002200	0.058699
4 ⁰	0.023825	0.145452	0.010114	0.061745
8 ⁰	0.060526	0.172135	0.025693	0.073072
12 ⁰	0.108989	0.199491	0.046266	0.084684

At minimum wind velocity, the aerodynamic forces are much lower. For example, at 0⁰ AOA, lift is 0.005183 N and drag is 0.138278 N while Cl and Cd are 0.002200 and 0.058699, respectively. At 12⁰ AOA, lift rises to 0.108989 N while drag increases to 0.199491 N, corresponding values for Cl and Cd being 0.046266 and 0.084684, respectively.

Table.8.Strain induced During Hovering

Throttle %	Compressive Strain ($\mu\text{m/m}$)
0	0.05
15	-13.22
25	-26.26
50	-92.71

The strain measurement process is facilitated by the use of the Mx1615B strain gauge amplifier and Catman software for data acquisition. These sophisticated tools enable the recording of compressive strain values at varying throttle levels during the hovering tests, as shown in Table 8. The compressive strain at 15% throttle is $-13.22\mu\text{m/m}$, and at 50%, the strain value rises sharply to $-92.71\mu\text{m/m}$. This experimental setup, meticulously designed and executed, demonstrates the effectiveness of using strain gauges for structural analysis of a hexacopter. This thorough approach ensures reliable performance evaluations while the hexacopter is in operation.

4. Conclusions

Numerical and experimental results of drag force, measured at wind speeds of 8.22 m/s, 5.81 m/s, and 3.68 m/s, are presented for different angles of attack (AoA). The highest drag force was observed when the Hexa-Copter exposed its maximum cross-sectional area to the airflow, a finding corroborated by CFD simulations of forward flight conditions and further validated through wind tunnel tests. The CFD models accurately predicted drag force by accounting for propeller rotation, while wind tunnel tests provided real-world measurements, confirming the computational predictions. The strong correlation between CFD and experimental results demonstrates the drone's aerodynamic stability and consistency in drag force values across varying wind speeds and AoA. This indicates that the Hexa-Copter configuration can maintain stable flights even under higher wind conditions, with CFD simulations reliably forecasting aerodynamic performance. The alignment between computational and experimental data highlights the critical importance of combining numerical simulations with physical testing for optimizing drone performance. The results affirm that the synergistic use of CFD simulations, wind tunnel tests, and advanced material designs significantly enhances the Hexa-Copter's aerodynamic stability and overall efficiency. This study underscores the ability of CFD simulations to predict aerodynamic performance for real-world applications and suggests that integrating computational predictions with experimental validation can guide further improvements in drone design, ensuring high performance and reliability under diverse flight conditions. The strain measurement process was conducted using the Mx1615B strain gauge amplifier and Catman software for data acquisition. These advanced tools facilitated the recording of compressive strain values at different throttle levels during hovering tests and compressive strain measured $-13.22\mu\text{m/m}$ at 15% throttle and increased sharply



to $-92.71 \mu\text{m/m}$ at 50% throttle. This designed experimental setup represents the effectiveness of strain gauges for structural analysis of the Hexa-Copter, ensuring reliable performance evaluations during operation.

References

1. Sharma, P., & Atkins, E. (2019). Experimental investigation of tractor and pusher hexacopter performance. *Journal of Aircraft*, 56(1), 1-15. <https://doi.org/10.2514/1.C035319>
2. Lei, Y., & Cheng, M. (2019). Aerodynamic performance of hex-rotor UAV considering the horizontal airflow. *Applied Sciences*, 9(22), 4797. <https://doi.org/10.3390/app9224797>
3. Kutty, H. A., & Rajendran, P. (2017). 3D CFD simulation and experimental validation of small APC slow flyer propeller blade. *Aerospace*, 4(10). <https://doi.org/10.3390/aerospace4010010>
4. Fasel, U., Keidel, D., Baumann, L., Cavolina, G., Eichenhofer, M., & Ermanni, P. (2020). Composite additive manufacturing of morphing aerospace structures. *Manufacturing Letters*, 23, 85-88.
5. Huang, Y., Tian, X., Li, W., He, S., Zhao, P., Hu, H., Jia, Q., & Luo, M. (2024). 3D printing of topologically optimized wing spar with continuous carbon fiber reinforced composites. *Composites Part B: Engineering*, 272, 111166.
6. Stamate, M.-A., Pupăză, C., Nicolescu, F.-A., & Moldoveanu, C.-E. (2023). Improvement of hexacopter UAVs attitude parameters employing control and decision support systems. *Sensors*, 23(3), 1446.
7. Marturano, F., Martellucci, L., Chierici, A., Malizia, A., Di Giovanni, D., d'Errico, F., Gaudio, P., & Ciparisse, J.-F. (2021). Numerical fluid dynamics simulation for drones' chemical detection. *Drones*, 5(3), 69.
8. Kulshreshtha, A., Gupta, S. K., & Singhal, P. (2020). FEM/CFD analysis of wings at different angles of attack. *Materials Today: Proceedings*, 26, 1638-1643.
9. Hiremath, S., & Malipatil, A. S. (2014). CFD simulations of aircraft body with different angles of attack and velocity. *International Journal of Innovative Research in Science, Engineering and Technology*, 3(10), 16965-16972.
10. Grant, S., Perine, J., Abi-Akar, F., Lane, T., Kent, B., Mohler, C., Scott, C., & Ritter, A. (2022). A wind-tunnel assessment of parameters that may impact spray drift during UAV pesticide application. *Drones*, 6(8), 204.
11. Al Rashid, A., Ikram, H., & Koç, M. (2022). Additive manufacturing and mechanical performance of carbon fiber reinforced Polyamide-6 composites. *Materials Today: Proceedings*, 62, 6359-6363.
12. Ning, F., Cong, W., Wei, J., Wang, S., & Zhang, M. (2015). Additive manufacturing of CFRP composites using fused deposition modeling: Effects of carbon fiber content and length. In *International Manufacturing Science and Engineering Conference* (Vol. 56826, p. V001T02A067). American Society of Mechanical Engineers.
13. Palomba, G., Crupi, V., & Epasto, G. (2022). Additively manufactured lightweight monitoring drones: Design and experimental investigation. *Polymer*, 241, 124557.
14. Cetinsoy, E., Hancer, C., Oner, K. T., Sirimoglu, E., & Unel, M. (2012). Aerodynamic design and characterization of a quad tilt-wing UAV via wind tunnel tests. *Journal of Aerospace Engineering*, 25(4), 574-587.



15. Moon, S. K., Tan, Y. E., Hwang, J., & Yoon, Y.-J. (2014). Application of 3D printing technology for designing light-weight unmanned aerial vehicle wing structures. *International Journal of Precision Engineering and Manufacturing-Green Technology*, 1, 223-228.
16. Daud, S. M. S. M., Yusof, M. Y. P., Heo, C. C., Khoo, L. S., Singh, M. K. C., Mahmood, M. S., & Nawawi, H. (2022). Applications of drone in disaster management: A scoping review. *Science & Justice*, 62(1), 30-42.
17. Hassanalian, M., & Abdelkefi, A. (2017). Classifications, applications, and design challenges of drones: A review. *Progress in Aerospace Sciences*, 91, 99-131.
18. Su, N., Pierce, R. S., Rudd, C., & Liu, X. (2022). Comprehensive investigation of reclaimed carbon fibre reinforced polyamide (rCF/PA) filaments and FDM printed composites. *Composites Part B: Engineering*, 233, 109646.
19. Parandha, S. M., & Li, Z. (2018). Design and analysis of 3D printed quadrotor frame. *International Advanced Research Journal in Science, Engineering and Technology*, 5(4), 66-73.
20. Zhu, H., Nie, H., Zhang, L., Wei, X., & Zhang, M. (2020). Design and assessment of octocopter drones with improved aerodynamic efficiency and performance. *Aerospace Science and Technology*, 106, 106206.
21. Nvss, S., Esakki, B., Yang, L.-J., Udayagiri, C., & Vepa, K. S. (2022). Design and development of unibody quadcopter structure using optimization and additive manufacturing techniques. *Designs*, 6(1), 8.
22. Do, T. D., Le, M. C., Nguyen, T. A., & Le, T. H. (2022). Effect of infill density and printing patterns on compressive strength of ABS, PLA, PLA-CF materials for FDM 3D printing. *Materials Science Forum*, 1068, 19-27.
23. Qu, J., Dong, Y., Gu, X., & He, S. (2022). Integrated frame topology optimization design of small quadrotor UAV. In *Journal of Physics: Conference Series* (Vol. 2292, No. 1, p. 012016). IOP Publishing.
24. Zhang, L., Dongli, M. A., Muqing, Y. A. N. G., Xinglu, X. I. A., & Yuan, Y. A. O. (2021). Optimization and analysis of composite sandwich box beam for solar drones. *Chinese Journal of Aeronautics*, 34(10), 148-165.
25. Edulakanti, S. R., & Ganguly, S. (2023). The emerging drone technology and the advancement of the Indian drone business industry. *The Journal of High Technology Management Research*, 34(2), 100464.
26. Öztürk, O. (2024). Parametric optimization of structural frame design for high payload hexacopter. *Black Sea Journal of Engineering and Science*, 7(5), 7-8.
27. Harvey, D., Villeneuve, E., Béland, M., & Lapalme, M. (2024). Wind tunnel investigation of the icing of a drone rotor in forward flight. *Drones*, 8(8), 380.
28. Baris, E., Britcher, C. P., & Altamirano, G. (2019). Wind tunnel testing of static and dynamic aerodynamic characteristics of a quadcopter. In *AIAA Aviation 2019 Forum* (p. 2973).
29. Wang, N., Li, X., & Yin, H. (2024). Trajectory tracking control for a hexacopter UAV: A constraint-following approach guaranteeing prescribed performance. *SAE Technical Paper*, 2024-01-7013.
30. Liu, Z. (2024). Functional integration design and aerodynamic characterization of a hexacopter agricultural unmanned aerial vehicle based on its appearance. *Frontiers in Mechanical Engineering*, 10, 1372010.



-
31. Joy, I. M. (2024). Computational fluid dynamics and aerodynamics-system identification of a real hexacopter for controlling the flight within urban environments.
 32. Sopegno, L., Pedone, S., Rutherford, M. J., Livreri, P., & Valavanis, K. P. (2024). Evaluation and comparison of state and disturbance observers for a terrestrial hexacopter. In *2024 International Conference on Unmanned Aircraft Systems (ICUAS)*, Chania - Crete, Greece (pp. 430-435). <https://doi.org/10.1109/ICUAS60882.2024.10557116>
 33. Vohra, D. S. (2024). Enhancing the total airborne duration for a quadcopter/hexacopter using tethered power cable/mechanism. In *2024 15th International Conference on Computing Communication and Networking Technologies (ICCCNT)*, Kamand, India (pp. 1-4). <https://doi.org/10.1109/ICCCNT61001.2024.10725768>
 34. Shelare, S., Belkhode, P., Nikam, K. C., et al. (2024). A payload-based detailed study on design and simulation of hexacopter drone. *International Journal of Interactive Design and Manufacturing*, *18*, 2675-2692. <https://doi.org/10.1007/s12008-023-01269-w>
 35. Beylergil, B., Tanoğlu, M., & Aktaş, E. (2020). Experimental and statistical analysis of carbon fiber/epoxy composites interleaved with nylon 6,6 nonwoven fabric interlayers. *Journal of Composite Materials*, *54*(27), 4173-4184. <https://doi.org/10.1177/0021998320927740>
 36. Feng, N., Wang, X., & Wu, D. (2013). Surface modification of recycled carbon fiber and its reinforcement effect on nylon 6 composites: Mechanical properties, morphology and crystallization behaviors. *Current Applied Physics*, *13*(9), 2038-2050. <https://doi.org/10.1016/j.cap.2013.09.009>
 37. Alessi, S., Di Filippo, M., Dispenza, C., Focarete, M. L., Gualandi, C., Palazzetti, R., Pitarresi, G., & Zucchelli, A. (2015). Effects of Nylon 6,6 nanofibrous mats on thermal properties and delamination behavior of high performance CFRP laminates. *Polymer Composites*, *36*(7), 1303-1313.